PCCP

Accepted Manuscript

ROYAL SOCIETY OF CHEMISTRY

www.rsc.org/pccp

PCCP

ARTICLE

Molecular dynamics of anhydrous glycolipid self-assembly in lamellar and hexagonal phases.

Received 00th January 20xx,
Accepted 00th January 20xx

DOI: 10.1039/x0xx00000x

www.rsc.org/

T.S. Velayutham*[a], H. S. Nguan[b,c], B. K. Ng[a], W. C. Gan[a], V. Manickam Achari[b], N. I. Zahid[b], W. H. Abd. Majid[a], C. Zannoni[d] , R. Hashim[b]

The molecular dynamics of a synthetic branched chain glycolipid, 2-decyl-tetradecyl-β-D-maltoside, ($C_{14\text{-}10}G_2$) in the dry assemblage of smectic and columnar liquid crystal phases has been studied by dielectric spectroscopy as a function of frequency and temperature during the cooling process. Strong relaxation modes were observed corresponding to the tilted smectic and columnar phases respectively. At low frequency (~900 Hz to 1 kHz) in the smectic phase, Process I* was observed due to the tilted sugar bilayer structure. The process continued in the columnar phase (Process I) with an abrupt dynamic change due to phase transition at the frequency range of ~1.3 kHz to 22 kHz. An additional process (Process II) was observed in the columnar phase with a broader relaxation at the frequency of ~ 10 Hz to 1 kHz. A bias field dependence study was performed in the columnar phase and we found that the relaxation strength rapidly decreased with increased applied dc bias field. This relaxation originates from a collective motion of polar groups within the columns. The results of the dielectric spectroscopy were supported with a molecular dynamics simulation study to identify the origin of the relaxation processes, which could be related to the chirality and hydrogen bond of the sugar lipid.

Introduction

Glycolipids (GLs) are one of three natural lipid components found in cell membranes, whose structure is often approximated to a simple two-dimensional bilayer in a liquid crystalline phase, embedding proteins.[1] Glycolipids are amphitropic, meaning they are able to self-assemble when dry as well as when solvated. The molecular structure of a glycolipid comprises a polar (hydrophilic) sugar headgroup and an apolar (hydrophobic) alkyl chain.[2] The nature of the alkyl chain and the type of sugar headgroup determine the phase behaviour when solvated (lyotropic) or in some cases even in dry anhydrous form, where changes of the molecular organization are purely driven by temperature (thermotropic). Both the biological membrane and the lyotropic phases have been studied extensively.[3, 4] However, their thermotropic phases have not been assessed with equal vigour and, in fact, interest in the thermotropic behaviour of glycolipids only began with the seminal work by Jeffrey et al. in 1986.[5] Even now, fundamental knowledge on the self-assembly of thermotropic glycolipids is scanty, hindering the serious investigation and development of possible thermotropic applications. Glycolipids have drawn much attention in recent years; for example, the sugar headgroup being chiral implies possible ferroelectric behaviour[6] associated with tilted structures (i.e. Smectic C (Sm C*)) instead of Sm A in the lipid organization.[7, 8] In addition, temperature-dependent electric polarization changes (pyroelectric effect) have been observed in this material.[9, 10] Moreover, cell membrane has been found to respond to an applied voltage, which implies possible piezoelectricity.[11]

Apart from the possibility of supporting the development of thermotropic applications from glycolipid mesophases, we have found that investigations in the anhydrous or dry state could provide ideas and lend support for the understanding of lyotropic phenomena. For example, our recent simulations of dry branched chain glycolipid have shown that hydrophobic alkyl chains are surprisingly able to probe into the hydrophilic region.[12] The association of hydrophilic head and the hydrophobic chain was at first unexpected, but sugar amphoteric nature made this possible, and the chain-sugar interaction has been observed previously.[13] Furthermore, the hydrophobic region in the headgroup may stimulate the formation of a "crack", should these chains leave the hydrophilic region. In the presence of water this crack will allow the former to flow into the hydrophobic region, creating the "water holes", as described by Gurtovenko and Vattulainen [14], in their molecular dynamics simulation, which demonstrated the lipid flip motion, a rare event in membrane transport phenomena but one thought to be related to cell apoptosis.

[a] Low Dimensional Materials Research Center, Faculty of Science, University Malaya, 50603 Kuala Lumpur, Malaysia. Fax: +60379674146; Tel: +60379674147; E-mail: t_selvi@um.edu.my
[b] Fundamental and Frontier Science of Self-Assembly Center, Faculty of Science, University Malaya, 50603 Kuala Lumpur, Malaysia.
[c] Institute of Atomic and Molecular Sciences, Academia Sinica, Taipei, Taiwan
[d] Dipartimento di Chimica Industriale "Toso Montanari" viale Risorgimento 4 Universita' di Bologna, 40136 Bologna, Italy.
See DOI: 10.1039/x0xx00000x

Recently, a new interesting class of synthetic glycosides with a branched chain design originated from Guerbet alcohols was prepared.[8] The properties of the phases obtained from these glycosides have been widely studied and reviewed.[8, 9] In particular, various fundamental investigations were carried out to assess potential applications of these Guerbet glycosides, both thermotropic and lyotropic.[7-10, 15] Many non-lamellar phases (for examples, hexagonal, ribbon, bicontinuous cubic phases, etc) observed from these glycosides in the dry state, suggest these phases may be stable in the corresponding lyotropic environment, from which nanoparticles such as hexasomes[16] and cubosomes[17] may be formulated for applications such as delivery systems.

Thermotropic studies by both Abeygunaratne et al.[7] and Liao et al.[8] using these Guerbet glycosides, also found a strong correlation between the number of sugar heads and the magnitude of the dielectric susceptibility, showing that the polar headgroups are very important for the field-induced polarization. A similar high susceptibility was observed in the so-called Goldstone mode of helical ferroelectric smectic C (S_C*) liquid crystals, suggesting these molecules may have a tilted chiral smectic instead of an orthogonal smectic or columnar phase.[7, 8] Glycolipid bilayer assemblages are usually thought to be in a Sm A phase, where the chains are randomized and fluid. Although chain tilting is not assumed for this phase, a recent computer simulation study suggested a possible tilted chain configuration. [18]

In a previous work, we have reported results for the molecular dynamics of three synthetic glycolipid thin films upon heating. [10] We found that the glycolipids with the shortest branched alkyl chain experience the most restricted self-assembly dynamic process compared to the longer chain, during the heating process. Among the glycolipids investigated, the one with the longest branched alky chain exhibits completely different mesophases during the cooling process. Thus, in the present investigation, the longer branched chain glycoside, 2-decyl-tetradecyl-β-D-maltoside, $C_{14\text{-}10}G_2$ with a wide mesophase range and displays possible polymorphism on cooling; columnar to smectic phases was studied. The orientation dependent response of the $C_{14\text{-}10}G_2$ compound was investigated using dielectric measurement in the presence of a biased field during the cooling process. The temperature response over a broad range of frequencies is used to characterize the nature of the molecular motion of the glycolipid in the smectic and columnar phases. A possible tilted structure was identified in the smectic phase, where there is a lateral correlation of molecular dipoles yielding a polar order within the layer. [7] Molecular dynamics simulations of the smectic (or bilayer) and of the columnar phases formed by the glycolipids were also conducted, in order to better understand the structure and dynamics of the molecules in these two liquid crystal phases.

Experimental

The detailed synthesis procedure for $C_{14\text{-}10}G_2$ was published elsewhere.[2, 8] The liquid crystalline phases were identified by polarizing microscopy using a Mettler Toledo FP82HT hot stage, and viewed with an Olympus BX51 microscope fitted with crossed polarizers. A magnification factor of 20x was used. The microscope was connected to an Olympus camera for image capture using AnalySIS® software for analysis.

For the dielectric measurement, the prepared $C_{14\text{-}10}G_2$ was dissolved in ethanol and successively immersed in an ultrasonic bath at 60 °C for 40 minutes to form a solution with a concentration of 0.5 g/ml. The solution was spin-coated (at 8000 rotations per minute for 10 s) onto a glass substrate, over which an aluminium electrode layer had been previously deposited by a thermal evaporation method, to produce a $C_{14\text{-}10}G_2$ thin film with a thickness of ~3 μm. A top electrode was deposited on the glycolipid $C_{14\text{-}10}G_2$ thin films to produce a metal-insulator-metal (MIM) structure with an active area of 2 mm x 2 mm. Dielectric measurements were carried out by using Agilent 4294A impedance analyser in the frequency range of 40 Hz to 1 MHz at cooling temperature from 443 K to 305 K on a hot chuck, which was controlled by an STC200 temperature controller. The measurement results were expressed in terms of complex dielectric permittivity ε^*

$$\varepsilon^* = \varepsilon' - i\varepsilon'' \quad (1)$$

where ε' and ε'' are the real and imaginary permittivity, respectively. In addition to conventional dielectric measurements, a dc bias field was superimposed to a sinusoidal electric field to examine its effects on the molecular ordering and dynamics of the glycolipid system.

We have also conducted an atomistic molecular dynamics computer simulation study using GROMACS, [19] in both the smectic and the columnar phases to understand the origin of the dynamic behaviour of this branched chain glycolipid $C_{14\text{-}10}G_2$ (see Fig. 1(a)). The molecule of $C_{14\text{-}10}G_2$ was modelled using the version 5.0.1 [20] united atoms (UA) force field, where each of the methine, methylene and methyl groups in the chain was coarse-grained into a single bead. Meanwhile the hydrogen atoms from the hydroxyl group within the sugar head were retained in the model (see Fig. 1 (b)). Within the GROMOS package, the united atom force field parameters for methine, methylene and methyl groups have been tuned so as to reproduce experimental results and have proved to be suitable for studying lipid aggregates such as membranes and micelles[20, 21]. In a recent simulation study,[22] a similar UA force field was applied to another member of the Guerbet glycoside $C_{12\text{-}8}G_1$ and the study was able to reproduce the hexagonal structural data reasonably in agreement with the small angle X-ray measurements.[23] This force field has the advantage of reducing the computational cost without compromising the capability of the model to represent the real molecules. Many other UA force field parameterization studies have been performed, some of which are able to reproduce the transition temperature of liquid crystalline materials[24] and the phase properties of gel and fluid lamellar structures in the membrane bilayer. [25]

Based on this glycolipid model, we have constructed the smectic and the columnar assemblies in a periodic box. For the double bilayer structure, initially a single monolayer was modelled using the crystal builder facility in HyperChem where the lipids are arranged in a 10 × 10 monolayer. Each monolayer was then geometry optimized and rotated by 180° and shifted to form a bilayer with the tail group of the molecules pointing toward each other at the centre of the bilayer and the headgroups facing opposite directions. The single bilayer was replicated to form a second bilayer, providing a large lamellar simulation cell of 200

lipids (see Fig. 5(a)). The initial structure of the bilayer was ordered and tilted so as to resemble the gel phase of the glycolipid that is usually found for such compounds at a lower temperature. Meanwhile, for the columnar structure, several $C_{14\text{-}10}G_2$ lipids were arranged into a disc with the headgroups pointing at the centre of the disc. Ten of these disc aggregates were stacked to form a column and the column was replicated and arranged into a hexagonal lattice containing 336 lipids (see Fig. 5(b)).

In both cases, the simulations were conducted with a constant number of particles N, the pressure P and temperature T (NPT), where N=10800 (for bilayer) and 18144 (for columnar), P = 1 atm. In addition the temperature of the smectic phase and the columnar phase were set to be T=348 K and 433 K, respectively. Periodic boundary conditions were applied and the integration of the Newtonian equations of motion was performed using the leap-frog algorithm with a time-step of 2 fs. In addition, a Linear Constraint Solver (LINCS) algorithm was used to fix the bond lengths involving the hydrogen atoms. The particle mesh Ewald (PME) approach was employed to calculate the electrostatic interactions with a cut-off of 12 Å. The cut-off of 12 Å was applied for the non-bonded interactions. The temperature was controlled by a Nose–Hoover thermostat, while the semi-anisotropic pressure coupling was applied to the bilayer structure and an isotropic pressure coupling was used for the columnar structure using Parrinello–Rahman pressure coupling. A similar computer simulation of aggregates like bilayer and hexagonal phase have been described and published elsewhere[18, 22]. In our current simulation work, the bilayer and columnar aggregates were used as the starting structures for the molecular dynamics (MD) simulations which we run for 300 ns each.

Results

Optical Polarizing Microscope

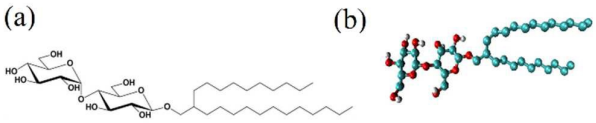

Fig. 1. 2-decyl-tetradecyl-β-D-maltoside ($C_{14\text{-}10}G_2$) (a) chemical structure in 3-D (b) united atom model structure

On cooling from the isotropic phase, the glycolipid $C_{14\text{-}10}G_2$ gave a columnar phase at 506 K and entered the smectic phase at 358 K. The smectic sample was cooled further up to 296 K. The representative textures of the smectic and columnar phases obtained are shown in Fig. 2. The fan-shape texture in the Fig. 2(a, b) indicates that the sample is in a smectic phase. However, when cooling the columnar phase into a smectic phase, a striated band texture was observed. The striated bands were not observed in the normal fan-shaped texture of the smectic phase obtained from heating of its crystalline phase (see Fig. 2(a, b). The striated bands in the texture (Fig. 2(b)) further suggests that it is possibly a smectic E, or a smectic C* or even a texture of a bent-core molecule [26]. Since the $C_{14\text{-}10}G_2$ molecule has a number of chiral centres and glycolipid chain tilting was observed in previous studies [7, 18], the possibility of a smectic E phase in this system is unlikely.

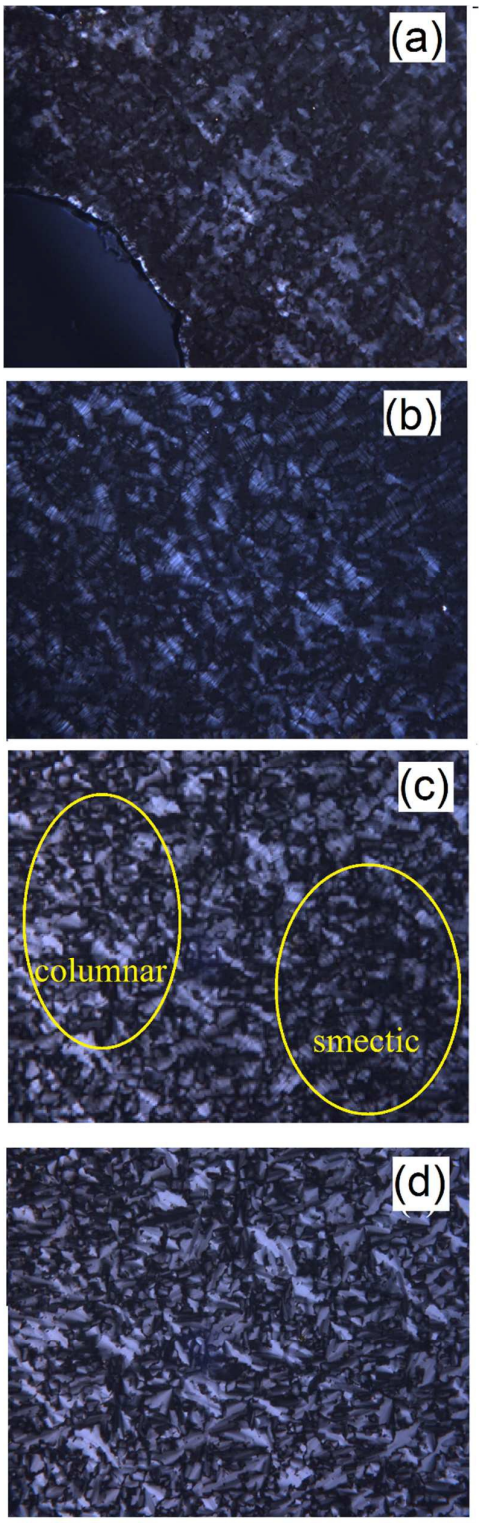

Fig. 2. OPM texture of (a) smectic phase during heating process (T=304 K); (b) smectic phase during cooling process (T=304 K) with banded fan-shape mimicking bent-core like structure; (c) phase transformation from columnar to tilted smectic phase (T= 358 K) marked by distinct regions; (d) columnar phase during cooling process (T=433 K). Magnification 20x.

The dark brushes of focal conic domains with some birefringence similar to biaxial bent-core molecule [27] can be considered as an evidence for the existence of tilted smectic phase (see Fig. 2(b)). We will discuss more on the structure of the smectic phase based on the dielectric spectroscopy and MD simulations in the later part of this manuscript. The columnar phase also produced a birefringence texture (refer to Fig. 2(c)); however the columnar phase tended to produce much larger domains than the smectic phase, as well as distinctly different optical textures consisting of leaf-type fan-shape domain typical of that from the thermotropic columnar phases [8].

Dielectric Studies

Generally, important information on the collective response of liquid crystal mesogens and their molecular properties can be deduced from their frequency dependent dielectric behaviour. The frequency spectra at different temperatures from 443 K to 305 K of the glycolipid are given in Fig. 3 where (a) shows the real permittivity, ε' and (b) the corresponding imaginary permittivity, ε'', respectively. The dielectric spectra, recorded for a large series of decreasing temperatures from T = 443 K to 305 K in steps of 1K, showed a decrease in intensity at each frequency upon cooling. In these figures, a gap (more obvious in (b)) between these constant temperature spectra can be seen at 361 K, corresponding to a phase transition from the columnar to the smectic phase. This transition temperature is in agreement (within the experimental error) with that observed by Optical Polarizing Microscope (OPM) at 358 K (refer to Fig. 2(c).

On cooling, two relaxation processes were observed in the columnar phase and one relaxation in the smectic phase (see Fig. 3(b)). The relaxation at higher frequencies (f ~ 22 kHz to ~ 1.3 kHz) in the columnar phase is assigned to Process I. This process continued in the smectic phase to become Process I* with an abrupt dynamic change due to the phase transition. Process I* relaxation frequency is observed at ~1200 Hz for 360 K. As the temperature was reduced gradually to room temperature the relaxation frequency shifted to ~900 Hz. Furthermore, in the columnar phase, another relaxation peak is observed at the lower frequencies in the range of ~10 Hz (443 K) to ~1 kHz (383 K) and this is assigned as Process II.

The dielectric strength, relaxation frequencies and the activation energies of every process were calculated by fitting the data to the following equation,

$$\varepsilon^* = \sum_k \varepsilon_k + \varepsilon_\infty + i\,\frac{\sigma_{dc}}{\omega^\gamma} \quad , \qquad (2)$$

where the angular frequency is defined as $\omega = 2\pi f$, σ_{dc} is the dc conductivity, ε_∞ is the instantaneous permittivity and γ is the parameter describing the distribution of relaxation times. For real systems there may be a number of contributions to the dielectric permittivity, each relaxing at a different frequency. Since the dielectric spectrum is composed of a few bands, the dielectric absorption is described as a sum of several bands using the Havriliak-Negami (HN) function, which is an empirical modification of the Debye relaxation model, accounting for the asymmetry and broadness of the dielectric dispersion curve. For each dielectric process, $\varepsilon_k(\omega)$ was fitted to the HN function:

$$\varepsilon_k = \sum_k \frac{\Delta\varepsilon_k}{((1+(i\omega\tau_k)^{\beta_k})^{\alpha_k}} \quad , \qquad (3)$$

where $\Delta\varepsilon$ and τ are the dielectric strength and relaxation time respectively. Both α and β are parameters controlling the distribution of relaxation times. The experimental data can be reproduced very well using Eq. 2 (the fitted curve is not shown here). In the columnar phase, the spectra are more complex. Process I has $\alpha \approx 0.8$ and $\beta \approx 0.8$ while Process II has broader spectra with a larger range of dielectric strength (~100 to 800). In the smectic phase (Process I*), the value $\alpha \approx 0.8$ at room temperature and increases to 0.95 at higher temperatures, while $\beta \approx 0.9$ reduces to 0.7.

The temperature dependence of the dielectric strength for the three processes is given in Fig. 3(c). The dielectric strength for Process I and I* ranges from 3 to 15 (blue scale) and this is smaller compared to that in Process II in the range of 150 to 800 (red scale). Overall, the dielectric strength decreases continuously during the cooling process for all the three relaxation modes. However, the dielectric strength decreases at a faster rate in Process II compared to the other processes. The dielectric strength for Process I decreases more gradually and becomes almost linear in Process I*. Although there is no significant jump across the phase transition between the columnar to the smectic phase (Process I to I*), a discernible kink can be observed (see Fig. 3(c)) at this point suggesting the reorientation of molecules about the long axis takes place during the phase transition from columnar to smectic phase [28].

Fig. 3(d) shows the log of the relaxation time versus the reciprocal of temperature for all three processes without bias field. The straight-line character of the log plots can be fitted with the Arrhenius law for all the three relaxation processes, with activation energies, E_a, 54±3 kJ/mol, 18±1 kJ/mol and 10±2 kJ/mol for Process I, Process II and the Process I*, respectively. Moreover, the relaxation frequencies show slight discontinuities at the phase transition temperature (Process I to I*). It is noteworthy that the activation energy of Process I*, which is in the smectic phase, is lower compared to those of the Process I and II. This is unusual since the smectic phase, which is a more ordered phase than columnar, might be expected to have higher activation energy, at least if the process involves an end to end tumbling of the molecules. However, this might not be the case, if the dipole is transversal with respect to the molecular long axis. Furthermore, in the previous study [10] the activation energy of Process I* (on heating) was found to be 156 kJ/mol which is much higher than that found in the present case obtained on cooling. Higher activation energy implies a greater hindrance to the molecular process [29]. These observations show that smectic phase obtained on cooling from the columnar phase may have a different structure compare to the smectic obtained on heating from crystalline phase. The low activation energy of Process I* (in the present study) is also found weakly dependent on increasing temperature.

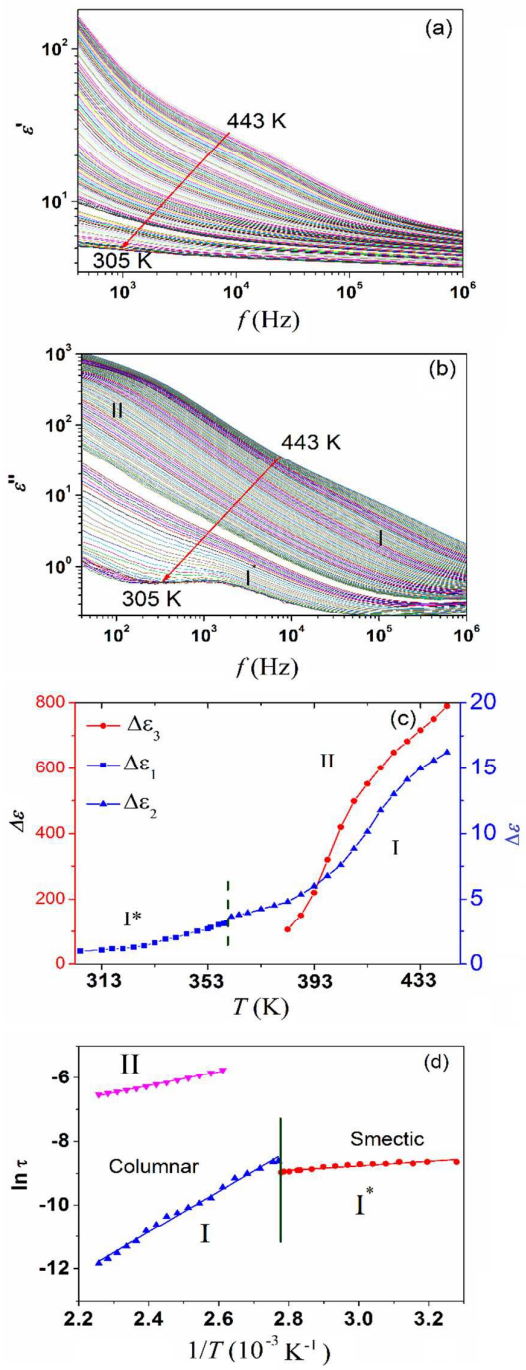

Fig. 3 Dielectric spectra of the glycolipid ($C_{14\text{-}10}G_2$) during a cooling process with a step of 1 K from 443–305 K; (a) for real permittivity (b) for imaginary permittivity. (c) The temperature dependence of the dielectric strength of the glycolipid. (d) Arrhenius plot of the relaxation processes involved. The relaxation processes are marked as I, I* and II.

The dielectric permittivity in the columnar phase at lower frequencies (Process II) is quite large, *ca.* 100, which suggests the presence of a strong positive dipolar correlation and dipole cooperative motions in the columnar phase. This prompted us to investigate the effect of dc bias field on these relaxation modes. When the bias field was applied, both Process I and I* were not affected but Process II was suppressed. Fig. 4 shows the results of the measurement at 403 K (columnar phase), where we have carefully subtracted a spurious contribution of the dc conductivity and electrode polarization from the experimental points. The bias field dependence of the real and imaginary permittivity is shown in Fig. 4(a) and (b), respectively. The dielectric strength, $\Delta\varepsilon$ obtained by fitting the experimental results with Eq. (2) is presented in Fig. 4(c). The results show $\Delta\varepsilon$ decreases as the bias field, E, increases in the columnar phase at the relaxation frequency of ~400 Hz. In addition, a dc bias field causes the relaxation frequency to slightly shift to a lower frequency. The dielectric strength is expected to be suppressed since the applied biased field will hinder the precession motion of the lipids in the plane of the columnar structure. In another study, two similar phenomena were observed for symmetric achiral bent-core liquid crystals system and 4-(2-methylbutyl)-phenyl-4'-(octyloxy)-(l,l')-biphenyl-carboxylate by Guo et al. and Pfeiffer et al., respectively [30, 31]. Similarly in ferroelectric SmC* the Goldstone mode corresponding to fluctuations of the polarization vector inside the cone, i.e. at constant tilt angle is suppressed by the bias field, while the soft mode corresponding to fluctuations in the tilt angle is relatively unaffected by the bias field [32].

Molecular Dynamics Simulation

Final simulated configurations (after 300ns) of the glycolipid assemblies in the smectic (side view) and hexagonal (top view) phases are given in Fig. 5. The structural properties of these two simulation systems, namely the local density profiles (LDPs) and the radial distribution functions (RDFs) are given in the supplementary material (see Fig. S1). The lattice parameter estimated from the simulations for the smectic phase is 3.80 nm, while that for the columnar phase is 3.46 nm. These lattice parameters are in a reasonable agreement with those obtained from the small angle X-ray measurements which gave 3.60 nm and 3.56 nm for smectic and columnar phase respectively[33, 34].

From our simulations of the smectic phase, we have observed a considerable tilting of the assembly consistent with the OPM texture of a tilted smectic shown in Fig. 2. We have shown a single configuration bilayer to illustrate the tilting effect in Fig. 6. Based on the structure of the $C_{14\text{-}10}G_2$ molecule, which has rather rigid, long and heavy maltose headgroup compared to its tails, we believe the tilting in each layer is a result of headgroup tilting. In our simulation, we defined an angle β, which is the angle between a vector connecting the O1' of the reducing sugar to the C4 of the non-reducing sugar of one headgroup layer (Fig 6(a)) and a similar vector from the sugar headgroup of the adjacent layer. If the headgroups of two adjacent layers are not tilted with respect to each other, the angle β will be 180°. In the initial structure the angle β was set to be 70°, but during the simulation the structure equilibrated and we found, over the last 200 ns of the MD simulation run, this angle became approximately 134° on average.

For the columnar phase at a temperature of 433 K, the thermal effects together with long simulation run removed the bias in the initial structure. This can be seen from the large variation of the

mean square displacement Δr^2 over time in the columnar phase, see Fig. S2(a) which gives the mean square displacement (MSD) of the lipid taken from an extended 100 ns run of the simulation. Furthermore, the diffusion of the molecules is following the Einstein diffusion equation such that $\Delta r^2 \propto t^{\gamma}$, where $\gamma = 1$. This linear relationship implies in the columnar phase glycolipid molecules do not experience significant over-crowding.

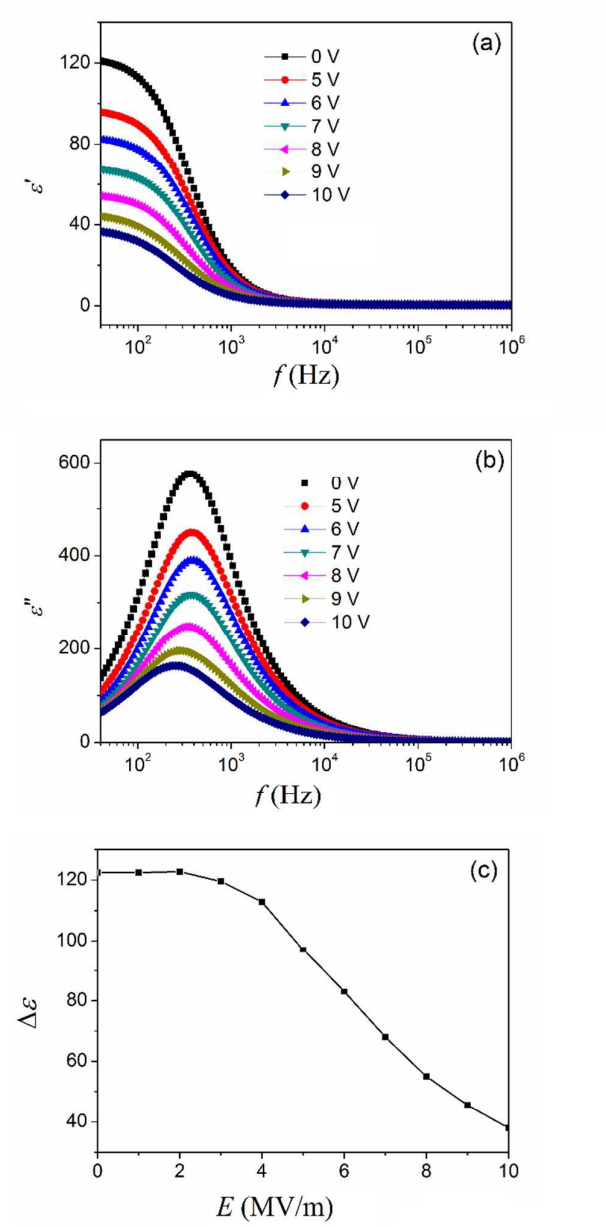

Fig. 4 Bias field dependence of (a) the real permittivity, (b) imaginary permittivity and (c) dielectric strength spectra for the glycolipid in the columnar phase at 403 K. The dielectric response strongly decreases by increasing the dc bias field.

On the other hand, in the smectic phase at lower temperature (T=348 K) anomalous diffusion was found (see Fig.S2 (a-b)) the relatively small MSD indicates that even over 100 ns the molecular motion was not enough to observe significant changes from its equilibrated structure. This anomalous behaviour ($\gamma < 1$) in the smectic phase is similar to those observed in the simulations of phospholipid bilayers by Jeong et al.[35]

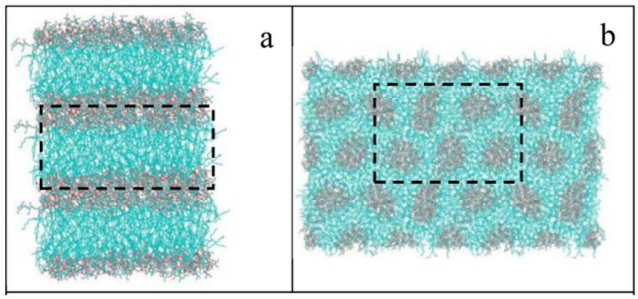

Fig. 5 The final equilibrium structures (after 300 ns) of the glycolipid $C_{14\text{-}10}G_2$ assemblies in (a) smectic and (b) columnar phases, from the molecular dynamic simulations. Dashed rectangles represent the original simulation boxes (unit cells) while those outside are the periodic images

Moreover, for the smectic phase we removed the bias in the initial structure by using the replica-exchange molecular dynamics (REMD) simulations method.[36] In our REMD simulation, a series of 20 smectic phase configurations, each with a different temperature in the range between 348–443 K with a 5 K increment, was run in parallel with an attempted configuration exchange every 1 ps according to the Monte Carlo acceptance-rejection rule. Through REMD simulation, the high-temperature configurations can exchange with the low-temperature ones, helping to prevent the system from being trapped in a local minimum of its free energy surface. We have run the REMD simulations for a further 25 ns with exchange probability between configurations of about 0.2. This proved effective in moving away from the initial configurations, as indicated by the significant changes in structural parameters.

The vectors representing the sugar headgroups (each defined in Fig. 6 (a)) in one typical simulation frame are shown in Fig. 6(b). These were found to be not only tilted but also shifted (see Fig. 6 (c)-(d)). Thus, within a single layer these glycolipid headgroups are tilted against the next adjacent headgroup layer, forming a shifted (twisted) V-configuration for the two layers in a manner similar to that of a bent-core liquid crystal [37]. The shifted V-configuration is due to the presence of a second angle, α defined by the angle between the projections of the tilt vectors onto the bilayer plane (Fig. 6(e)). From the simulation the angle α is estimated to be about 64°, compared to that of our initial structure which is only 9°. Therefore, the simulation results indicate that the polar molecules prefer to be tilted with respect to the layer normal without cancelling the polarization of the next layer.

In the smectic phase produced by the REMD method, we find that the angles α and β fluctuate between 30°~100° and 129°~160°, respectively (see the plot over the last 20ns in the Supplementary Fig. S3). Throughout the last 20ns of REMD simulation, arrangements of glycolipid molecules similar to those shown in Fig. 6 (b) are observed for system with temperature 348 K. Meanwhile at higher temperatures the orientations of sugar heads

in the smectic phase gradually become more randomized (see supplementary Fig. S4).

In contrast, the average tilt angle θ (which is the angle made by the sugar head vector with the column axis) of the glycolipids fluctuates around 90°, which indicates that there is no preferred average tilt away from the radial arrangement in the columnar phase (see supplementary Fig. S5).

Discussion

From both the dielectric spectroscopy and the simulation results, we assign the different relaxation processes observed as follows. On cooling the glycolipid $C_{14\text{-}10}G_2$, in the columnar phase, over the whole temperature range investigated, two relaxation modes (Process I and II) were observed. The low-frequency absorption (Process II) has a large intensity and its dielectric strength reduces with decreasing temperature. Process II involves slower dynamics (i.e. lower frequency), and its activation energy, *ca.* 18 kJ/mol is smaller compared to Process I. Since the sugar headgroups' meet at an angle (θ) of about 90° with respect to the column axis as can be seen from the simulation (Fig. S5), the columnar phase of these sugar lipids, will be made of stacked discs. Thus, from such structure, an extra cooperative motion may be perceived (Fig. 7a).

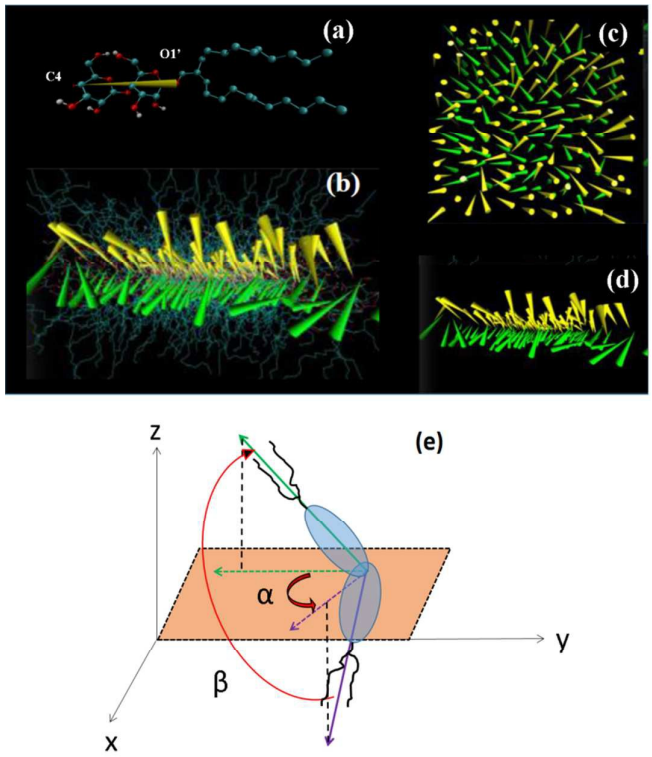

Fig. 6 Headgroup tilting of $C_{14\text{-}10}G_2$ in the two inner layers (L2 and L3). (a) Definition of a vector O1' to C4 within a single headgroup. (b) Distribution of these vectors within the two bilayers in a single snapshot. The vector distribution without the lipid from the top view (c) and side view (d). (e) Definitions of two tilt angles β and α. The angle between these two vectors is β, and α is the angle between the projections of these vectors on the lipid plane.

Moreover, for a collective motion that contributes to the dielectric relaxation, the precondition should be the existence of a significantly high spontaneous polarization, which is the sum of a large number of molecular dipole moments. For individual molecules we can estimate the strength of dipole moment and its direction through quantum mechanical calculation at a theory level which is expected to be reliable and accurate. Here we employ density functional theory (DFT) at the B3LYP level with 6-31G(d) basis set as implemented in Gaussian O9[38]. The single molecule dipole moment we obtain from the DFT method is 4.2 Debye, while its orientation is almost orthogonal to its molecular axis.

Considering one single column of molecules in the columnar phase, the column has a C_∞ rotational symmetry axis along the column axis. Therefore the total dipole in a direction perpendicular to the C_∞ axis should be cancelled off. However, glycolipid is a chiral molecule and lacks a mirror plane symmetry perpendicular to the columnar axis. Consequently, there will be a net dipole along the columnar axis. In principle, this net dipole reorientation should be the reason for the collective motion under the influence of the electric field.

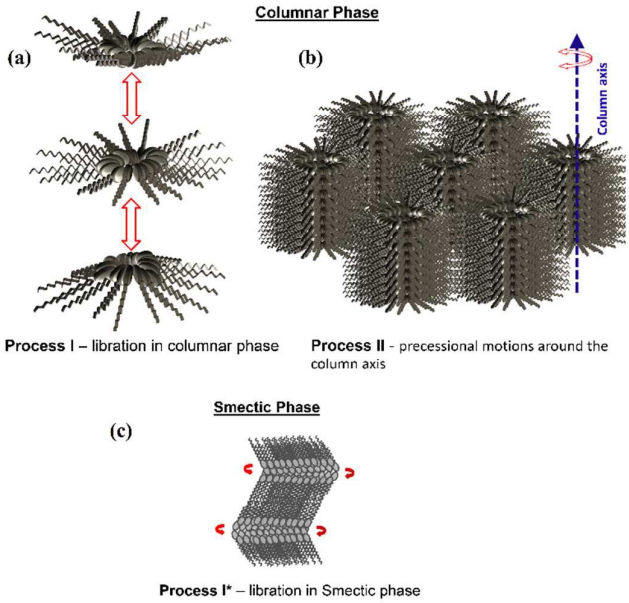

Fig. 7 A schematic diagram of the (a) Process I and II in the thermotropic columnar phase and (b) Process I* in the smectic phase. Process II is suspected to be either precessional motion around the column axis or the fanning of the disk.

Furthermore, the dc-bias field experiment supports the assignment where the relaxation frequency decreased, simultaneously with decreasing dielectric strength, under increasing bias field (as shown in Fig. 4). This phenomenon is similar to that observed by Guo et al., [30], for the bent shaped compounds showing distinct polar orthogonal phase, SmA_dP_A (interdigitated layer structure and antiferroelectric order) due to partial distortion of antiferroelectric order in adjacent layers leading to the stimulation

of non-compensated polarization. Generally, the relaxation originating from the non-collective movement of molecular dipoles is hardly influenced by a dc bias field.

On further cooling to below 358 K, a smectic layered structure was observed and confirmed by both OPM and the dielectric spectroscopy measurements, with only one low-frequency relaxation mode assigned to be Process I*. The OPM texture appears to be striated which implies a bent-core texture possibly derived from the tilted structure. The tilted smectic structure is confirmed by the simulation study where it was observed, as already discussed, that the sugar units of adjacent layers met at an angle β different from 180°. In fact β=134° and a further additional angle α=64° was also observed, implying a slight twist in the sugar head region.

The observation from the simulation study is rather unusual and unexpected since sugar lipids, despite containing many chiral centres, do not form a chiral smectic phase with helical directors [39]. The reason for this is the presence of strong hydrogen bonds which prevent the structure to twist so that its local directors could distribute into a helix. However, it does not even form a normal smectic A phase. Therefore, we believe that the observed bent and twisted structure of the smectic layers (Fig. 6) is the result of a competition between the chiral and the hydrogen bond interactions.

The presence of two competing forces could explain the relaxation Processes I and I* observed in both the columnar and smectic phases respectively from the dielectric spectroscopic measurement. Thus, Process I and I* could be attributed to the libration motion of the sugar headgroups to accommodate the two opposing forces. (See Fig. 7b)

The experimental results also show lower dielectric strength (~3 –5) and activation energy (10 kJ/mol) in the smectic phase compared to columnar phase. Furthermore, both quantities are much lower compared to the smectic phase on heating (Δε= ~1300; activation energy ≈ 134 kJ/mol) [10] as previously reported. Although further investigations would be needed to include other possibilities, it seems that there is some ferroelectric-like building up of the dipoles, probably connected with the chirality and that in the tilted smectic at a lower temperature the build-up is blocked by the onset of the hydrogen bond network.

Conclusions

We have studied in detail some structure and dynamics of glycolipid self-assembly of a Guerbet maltoside $C_{14\text{-}10}G_2$, which gives both smectic and columnar phases during the cooling cycle, by using dielectric spectroscopy and molecular dynamics (MD) simulation. Based on its dielectric properties and MD simulations, the smectic phase of $C_{14\text{-}10}G_2$ which give the OPM texture of fan-shape with the striated band, was assigned to tilted smectic phase. In the columnar phase, the dielectric spectrum gives two relaxation peaks (Process II and I). Process II is related to the precession motion about the column axis of the stacked discs. The assignment of Process II was confirmed by the bias field experiment where it was suppressed by the applied field. Process I of the columnar phase is related to the smectic phase (Process I*) which was observed on further cooling. These processes involve librational motions of the bent sugar units in the smectic and columnar phases as a result of the competition of chirality and hydrogen bond. The conformational dynamics involved in this glycolipid should enable one to detect multiple sub-states of the segment of glycolipid molecules in different phases. Furthermore, the tilting behaviour of the glycolipid assemblies in smectic phase may provide the basis for understanding "bio-ferroelectricity" phenomenon in the cell membrane.

Acknowledgements

This work was partially supported by University of Malaya under the High Impact Research Grant UM.C/625/1/HIR/166 and UMRG Grant RP026D-15AFR, by the Higher Ministry of Education under High Impact Research Grant (UM.C/625/1/HIR/MOHE/05). The authors wish to thank Professor Takeo Furukawa (Kobayashi Institute of Physical Research, Japan) for his valuable exchanges.

Notes and references

1. K. Holmberg, *Curr. Opin. Colloid Interface Sci.*, 2001, **6**, 148–159.
2. R. Hashim, A. Sugimura, H. Minamikawa and T. Heidelberg, *Liq. Cryst.*, 2012, **39**, 1-17.
3. P. Mattjus, *Biochim. Biophys. Acta (BBA)*, 2009, **1788**, 267-272.
4. M. Hato, H. Minamikawa, K. Tamada, T. Baba and Y. Tanabe, *Adv. Colloid Interface Sci.*, 1999, **80**, 233-270.
5. G. A. Jeffrey and H. Maluszynska, *Carbohydr. Res.*, 1990, **207**, 211-219.
6. V. Vill, F. Fischer and J. Thiem, *Z. Naturforsch.*, 1988, **43a**.
7. S. Abeygunaratne, R. Hashim and V. Vill, *Phys. Rev. E*, 2006, **73**, 011916.
8. G. Liao, S. K. Zewe, J. Hagerty, R. Hashim, S. Abeygunaratne, V. Vill and A. Ja´kli, *Liq. Cryst.*, 2006, **33**, 361–366.
9. B. Ng, T. Velayutham, W. Gan, W. A. Majid, V. Periasamy, R. Hashim and N. M. Zahid, *Ferroelectrics*, 2013, **445**, 67-73.
10. T. S. Velayutham, B. K. Ng, W. C. Gan, W. H. A. Majid, R. Hashim, N. I. Zahid and J. Chaiprapa, *J. Chem. Phys*, 2014, **141**, 085101.
11. I. Tasaki and K. Iwasa, *Jpn. J. Physiol.*, 1982, **32**, 505-518.
12. V. ManickamAchari, R. A. Bryce and R. Hashim, *PLoS ONE*, 2014, **9**, e101110.
13. C. Chen, D. Berns and A. Berns, *Biophys. J.*, 1981, **36**, 359-367.
14. A. A. Gurtovenko and I. Vattulainen, *J. Phys. Chem. B*, 2007, **111**, 13554-13559.
15. N. J. Brooks, H. A. A. Hamid, R. Hashim, T. Heidelberg, J. M. Seddon, C. E. Conn, S. M. Mirzadeh Husseini, N. I. Zahid and R. S. D. Hussen, *Liq. Cryst.*, 2011, **38**, 11-12.
16. N. Ahmad, R. Ramsch, J. Esquena, C. Solans, H. A. Tajuddin and R. Hashim, *Langmuir*, 2012, **28**, 2395-2403.
17. M. Salim, N. I. Zahid, C. Y. Liew and R. Hashim, *Liq. Cryst.*, 2016, **43**, 168-174.

18. V. Manickam Achari, H. S. Nguan, T. Heidelberg, R. A. Bryce and R. Hashim, *J. Phys. Chem. B*, 2012, **116**, 11626-11634.
19. D. Van Der Spoel, E. Lindahl, B. Hess, G. Groenhof, A. E. Mark and H. J. Berendsen, *J. Comput. Chem.*, 2005, **26**, 1701-1718.
20. C. Oostenbrink, A. Villa, A. E. Mark and W. F. Van Gunsteren, *J. Comput. Chem.*, 2004, **25**, 1656-1676.
21. L. D. Schuler, X. Daura and W. F. Van Gunsteren, *J. Comput. Chem.*, 2001, **22**, 1205-1218.
22. H. Nguan, S. Ahmadi and R. Hashim, *Phys. Chem. Chem. Phys.*, 2014, **16**, 324-334.
23. H. A. Hamid, R. Hashim, J. M. Seddon and N. J. Brooks, *Adv. Mater. Res.*, 2014, **895**, 111-115.
24. G. Tiberio, L. Muccioli, R. Berardi and C. Zannoni, *ChemPhysChem*, 2009, **10**, 125-136.
25. R. Tjörnhammar and O. Edholm, *J. Chem. Theory Comput.*, 2014, **10**, 5706-5715.
26. I. Dierking, *Textures of liquid crystals*, John Wiley & Sons, 2006.
27. M. W. Schröder, S. Diele, G. Pelzl, N. Pancenko and W. Weissflog, *Liq. Cryst.*, 2002, **29**, 1039-1046.
28. H. Takezoe, K. Kishikawa and E. Gorecka, *J. Mater. Chem.*, 2006, **16**, 2412-2416.
29. P. Salamon, N. Éber, Á. Buka, J. T. Gleeson, S. Sprunt and A. Jákli, *Phys. Rev. E*, 2010, **81**, 031711.
30. L. Guo, K. Gomola, E. Gorecka, D. Pociecha, S. Dhara, F. Araoka, K. Ishikawa and H. Takezoe, *Soft Matter*, 2011, **7**, 2895-2899.
31. M. Pfeiffer, S. Wrobel, L. A. Beresnev and W. Haase, *Mol. Cryst. Liq. Cryst.*, 1991, **202**, 193-206.
32. S. U. Vallerien, F. Kremer, H. Kapitza, R. Zentel and W. Frank, *Phys. Lett. A*, 1989, **138**, 219-222.
33. H. S. Nguan, T. Heidelberg, R. Hashim and G. J. T. Tiddy, *Liq. Cryst.*, 2010, **37**, 1205-1213.
34. R. Hashim, H. H. A. Hashim, N. Z. M. Rodzi, R. S. D. Hussen and T. Heidelberg, *Thin Solid Films*, 2006, **509**, 27-35.
35. J.-H. Jeon, H. M.-S. Monne, M. Javanainen and R. Metzler, *Phys. Rev. Lett.*, 2012, **109**, 188103.
36. C.-Y. Lin, C.-K. Hu and U. H. E. Hansmann, *Proteins: Structure, Function, and Bioinformatics*, 2003, **52**, 436-445.
37. J. Ortega, C. L. Folcia, J. Etxebarria, N. Gimeno and M. B. Ros, *Phys. Rev. E*, 2003, **68**, 011707.
38. M. Frisch, G. Trucks and H. Schlegel, *Inc., Wallingford, CT*, 2009.
39. H. A. van Doren, E. Smits, J. M. Pestman, J. B. F. N. Engberts and R. M. Kellogg, *Chem. Soc. Rev.*, 2000, **29**, 183-199.